Constrained polarization demultiplexing for coherent optical receivers

Ioannis Roudas[(1)], Athanasios Vgenis[(1)], Constantinos S. Petrou[(1)], Yihong Mauro[(2)], Srikanth Raghavan[(2)], and Lampros Raptis

[(1)] Dept. of Electrical and Computer Engineering, University of Patras, Greece; roudas@ece.upatras.gr
[(2)] Corning Inc., Corning, NY 14831, USA; raghavans@corning.com

This research project is co-financed by E.U.-European Social Fund (75%) and the Greek Ministry of Development-GSRT (25%).

Abstract Blind electronic polarization demultiplexing in coherent optical receivers using the constant modulus algorithm occasionally suffers from singularities. The introduction of constraints in the polarization demultiplexer's transfer function compensates for this deficiency, greatly enhancing convergence speed.

Introduction

Polarization demultiplexing in polarization-diversity coherent optical receivers can be performed electronically, using a two-input/two-output adaptive filter with four complex taps [1]-[7]. The constant modulus algorithm (CMA) [8] is a good candidate for adaptation of the demultiplexer taps due to its low computational complexity and its robustness in the presence of intermediate frequency (IF) offsets and laser phase noise [5]. However, its major shortcoming is its possible erroneous convergence to the same polarization tributary [6]-[7].

To remedy this problem, Kikuchi [6] proposed an enhanced CMA polarization demultiplexer with constraints on its taps. Elaborating on Kikuchi's idea, we propose a new zero-forcing constrained polarization demultiplexer. Its transfer matrix, in the absence of polarization mode dispersion (PMD) and polarization dependent loss (PDL), can be expressed as a function of only two real parameters (as opposed to two complex parameters in [6]). We study, by simulation, the convergence properties and the performance of the proposed polarization demultiplexer in PDM quadrature phase shift keying (QPSK) coherent optical systems. We prove that convergence is always guaranteed and is achieved considerably faster than with its conventional counterpart [5].

A rudimentary intradyne receiver with the proposed polarization demultiplexer can be used in order to theoretically estimate the tolerance of uncompensated coherent optical communications systems to PMD and PDL. Furthermore, it can be also used as a benchmark for comparing the performance of more sophisticated electronic adaptive PMD/PDL equalizers [9].

Constrained CMA polarization demultiplexer

The block diagram of a polarization- and phase-diversity coherent intradyne synchronous receiver is shown in Fig. 1(a) [10]. The receiver front-end is composed of a local oscillator (LO), two polarization beam splitters (PBS), two 2×4, 90° optical hybrids, and four balanced detectors (BRx). The four photocurrents are low-pass filtered (LPF), sampled by an analog-to-digital converter, and processed using a digital application-specific integrated circuit (DSP).

The received complex electric field vector $\mathbf{E}(t)$ can be written as $\mathbf{E}(t)=E_s(t)\left|e_s(t)\right\rangle+E_p(t)\left|e_p(t)\right\rangle$, in equivalent baseband notation. In the above, $E_s(t),E_p(t)$ denote the complex envelopes of the PDM QPSK signals, and $\left|e_s(t)\right\rangle,\left|e_p(t)\right\rangle$, are slowly-varying normalized Jones vectors [11], [12] along two arbitrary orthogonal states of

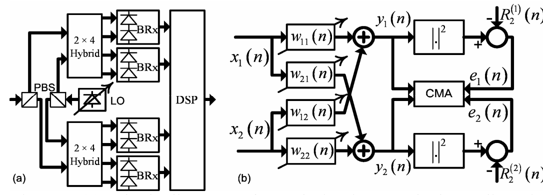

Fig. 1. (a) Block diagram of a polarization- and phase-diversity coherent intradyne synchronous receiver; (b) Block diagram of the proposed CMA polarization demultiplexer.

polarization (SOPs). The latter can be expressed in terms of the azimuth $\alpha(t)$ and ellipticity $\varepsilon(t)$ of $\left|e_s(t)\right\rangle$ [11].

The photocurrents at the output of the four balanced receivers are sampled at integer multiples of the symbol period nT_s and combined, via complex addition, to form discrete-time scaled replicas $x_1(n),x_2(n)$ of the received complex electric field vector. The combined action of polarization rotations in optical fibers and of the optoelectronic conversion at the polarization- and phase-diversity coherent receiver front-end can be mathematically described by the equation $\mathbf{X}(n)=\mathbf{H}(n)\mathbf{U}(n)+\mathbf{N}(n)$. In the above, we defined the column-vectors of the scalar input signals $\mathbf{U}(n)=\left[u_1(n)\quad u_2(n)\right]^{\mathrm{T}}=\left[E_s(n)\quad E_p(n)\right]^{\mathrm{T}}$, of the complex photocurrents at the two polarization branches $\mathbf{X}(n)=\left[x_1(n)\quad x_2(n)\right]^{\mathrm{T}}$, and of the photocurrent noises $\mathbf{N}(n)=\left[n_1(n)\quad n_2(n)\right]^{\mathrm{T}}$, where T denotes transposition. The elements $n_1(n),n_2(n)$ are independent, identically-distributed (i.i.d), complex Gaussian noises with zero mean and variance σ^2. The channel transfer function $\mathbf{H}(n)$ is a unitary matrix [11] depending on $\alpha(t)$, $\varepsilon(t)$, exclusively.

The block diagram of the proposed CMA polarization demultiplexer is shown in Fig. 1(b). It performs a matrix multiplication $\mathbf{Y}(n)=\mathbf{W}(n)\mathbf{X}(n)$, where we have defined the column-vector of the output signals $\mathbf{Y}(n)=\left[y_1(n)\quad y_2(n)\right]^{\mathrm{T}}$ and the transfer function of the polarization demultiplexer as a 2×2 matrix $\mathbf{W}(n)$. We *deliberately constrain* the elements of $\mathbf{W}(n)$ to the form $\mathbf{W}(n)=\mathbf{H}^{\dagger}(n)$, where † denotes the adjoint matrix. Thus, the elements of $\mathbf{W}(n)$ are functions of only two independent parameters $\hat{\alpha}(n),\hat{\varepsilon}(n)$, which are estimates of $\alpha(n),\varepsilon(n)$. In contrast, the unconstrained CMA polarization demultiplexer [5] has eight independent

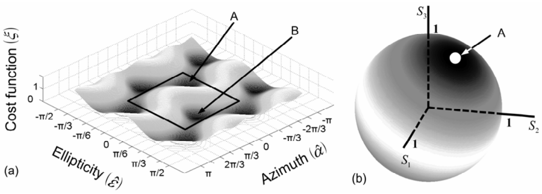

Fig. 2. (a) Three-dimensional plot of the cost function vs. estimated azimuth and ellipticity $\hat{\alpha}, \hat{\varepsilon}$. (Symbols: A, B: Global minima within the unit cell, Rectangle: Unit cell), (b) Corresponding contour plot of the cost function on the Poincaré sphere. (Symbols: White point (A): Minimum at $\hat{\alpha} = \hat{\varepsilon} = \pi/6$). (Conditions: Received SOP parameters: $\alpha = \varepsilon = \pi/6$). (Colors: Black: Small values, White: Large values of the cost function).

parameters (i.e., four complex coefficients $w_{ij},\ i, j = 1, 2$, with independent real and imaginary parts).

The parameters $\hat{\alpha}(n), \hat{\varepsilon}(n)$, are estimated using the CMA as follows: First, we define two distinct error functions $e_i(n) = |y_i(n)|^2 - R_2^{(i)},\ i = 1, 2$, where $R_2^{(i)},\ i = 1, 2$ are the sums of the average powers of the optical signals and the noise at each SOP, respectively. The cost function, which we seek to minimize, can be defined as the total mean-squared error [8] $\xi = E\left\{\Sigma_{i=1}^{2} e_i^2(n)\right\}$, where $E\{.\}$ denotes expectation. In matrix form, the error functions are written $\mathscr{E}(n) = \mathbf{Y}^*(n) \bullet \mathbf{Y}(n) - \Lambda$, where star denotes the complex conjugate, $\bullet$ denotes the Hadamard product, and $\Lambda = \left[R_2^{(1)} \quad R_2^{(2)}\right]^{\mathrm{T}}$. The instantaneous cost function is written $\xi(n) = \mathscr{E}^{\mathrm{T}}(n)\mathscr{E}(n)$.

For the adaptation scheme, we define an auxiliary column vector with elements equal to the independent parameters $\mathbf{Z}(n) = \left[z_1(n) \quad z_2(n)\right]^{\mathrm{T}} = \left[\hat{\alpha}(n) \quad \hat{\varepsilon}(n)\right]^{\mathrm{T}}$. The derivatives of the instantaneous cost function are

$$\begin{aligned}\partial\xi(n)/\partial z_j = 2\mathbf{E}^{\mathrm{T}}(n)\{&\mathbf{Y}^*(n) \bullet [\partial\mathbf{W}(n)/\partial z_j \mathbf{X}(n)] \\ &+ \mathbf{Y}(n) \bullet [\partial\mathbf{W}^*(n)/\partial z_j \mathbf{X}^*(n)]\}, \quad j = 1, 2\end{aligned} \tag{1}$$

The gradient of the instantaneous cost function is $\nabla\xi(n) = \left[\partial\xi(n)/\partial z_1 \quad \partial\xi(n)/\partial z_2\right]^{\mathrm{T}}$. Using the method of steepest descent [8], the recursive expression for updating the proposed CMA polarization demultiplexer coefficients is written $\mathbf{Z}(n+1) = \mathbf{Z}(n) - \mu\nabla\xi(n)$, where μ is a positive real constant (step-size parameter). Using periodic boundary conditions, the parameters $\hat{\alpha}(n)$ and $\hat{\varepsilon}(n)$ are confined within a unit cell, i.e., $|\hat{\alpha}| \le \pi/2,\ |\hat{\varepsilon}| \le \pi/4$.

Results and discussion

Fig. 2 (a), (b) show three-dimensional and Poincaré sphere-contour plots, respectively, of the cost function ξ vs. $\hat{\alpha},\ \hat{\varepsilon}$, in the absence of noise. In Fig. 2 (a) we observe that, within the limits of the unit cell, denoted by a rectangle, there are two global minima. In Fig. 2 (b), these minima correspond to two antipodal points on the Poincaré sphere. This indicates that the proposed polarization demultiplexer suffers from an output permutation ambiguity, i.e., the ordering of polarization tributaries at the demultiplexer outputs is arbitrary. This is a common feature of all CMA polarization demultiplexers [6]. The area surrounding each minimum corresponds to a valley within the unit cell of Fig. 2 (a). The intersection of the plane with the sphere creates a rotated equator, which corresponds to the ridge in the unit cell of Fig. 2 (a). The proposed algorithm will converge to the minimum lying in the same hemisphere as the initialization point corresponding to $\hat{\alpha}(0),\ \hat{\varepsilon}(0)$.

Fig. 3 (a), (b) show representative input/output constellation diagrams obtained by using the constrained and the conventional CMA polarization demultiplexers, respectively. We see that both polarization demultiplexers are able to transform the received amorphous constellation (drawn in blue) into four approximately circular points (in red) that resemble the transmitted constellation (green crosses). The recovered constellations immediately after the polarization demultiplexer might exhibit arbitrary rotations from their nominal position (rotation ambiguity) but this can be readily corrected by the feed-forward phase noise estimation circuit [10]. Fig. 3 (c) shows bit error rate (BER) curves as a function of optical signal-to-noise ratio (OSNR), for both CMA polarization demultiplexers. The BER is calculated using Monte Carlo simulation. Obviously, both CMA polarization demultiplexers exhibit almost identical performance with a small penalty of about 0.5 dB relatively to the ideal case. However, the constrained CMA polarization demultiplexer is considerably faster than [5]. For example, the constrained CMA polarization demultiplexer requires less than 20 symbol intervals to achieve $\xi(n) \cong 0$, while its conventional counterpart [5] requires more than 60 symbol intervals, i.e., a three-fold increase in convergence speed.

In summary, we proposed and studied, by simulation, a novel constrained CMA polarization demultiplexer for coherent optical receivers, which is superior to its conventional counterpart [5], in terms of convergence.

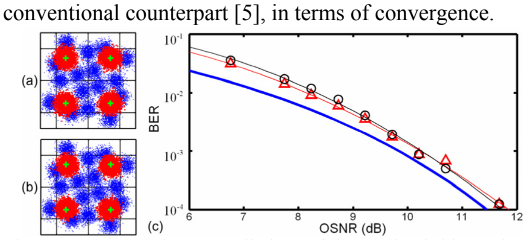

Fig. 3. Representative constellations of the received (blue points), equalized (red points) and ideal (green crosses) signals for the X polarization, using (a) the proposed constrained CMA polarization demultiplexer, and (b) the conventional CMA polarization demultiplexer [5]; (c) BER vs. OSNR for the ideal (i.e., distortionless) case (blue curve), the constrained (red triangles) and the conventional (black circles) CMA polarization demultiplexer. (Conditions: Received SOP parameters: α =π/6 and ε =π/12, resolution bandwidth $B_o \cong 1.25/T_s$).

References

[1] M. Tseytlin et al., *OFC*, MF83, Atlanta, GA, Mar. 2003.
[2] S. Calabrò et al., *ECOC*, vol. 4, pp. 950–951, Sep. 2003.
[3] R. Noé, *J. Lightw. Technol.*, vol. 23, pp. 802–808, Feb. 2005.
[4] Y. Han et al., *Opt. Expr.*, vol. 13, pp. 7527–7534, Sept. 2005.
[5] A. Leven et al., *OFC*, OTuO2, Anaheim, CA, Feb. 2008.
[6] K. Kikuchi, *LEOS Sum. Top.*, MC2.2, Mexico, Jul. 2008.
[7] H. Zhang et al., *ECOC*, Mo.3.D.5, Belgium, Sept. 2008.
[8] S. Haykin, *Adaptive Filter Theory*, Prentice-Hall, 1996.
[9] S. J. Savory, *Opt. Expr.*, vol. 16, pp. 804–817, Jan. 2008.
[10] K. Kikuchi, *Opt. Fiber Telecom.*, vol. VB, ch. 3, pp. 95–129.
[11] S. Huard, *Polarization of Light.*, Wiley, 1997, ch. 2.
[12] J. P. Gordon et al., *PNAS*, vol. 97, pp. 4541–4550, Apr. 2000.